Journal of
Applied Remote Sensing

Assessment of the spectral stability of Libya 4, Libya 1, and Mauritania 2 sites using Earth Observing One Hyperion

Taeyoung Choi
Xiaoxiong Xiong
Amit Angal
Gyanesh Chander
John J. Qu

SPIE

Downloaded From: http://remotesensing.spiedigitallibrary.org/ on 04/18/2016 Terms of Use: http://spiedigitallibrary.org/ss/TermsOfUse.aspx

Assessment of the spectral stability of Libya 4, Libya 1, and Mauritania 2 sites using Earth Observing One Hyperion

Taeyoung Choi,[a,*] Xiaoxiong Xiong,[b] Amit Angal,[c] Gyanesh Chander,[d] and John J. Qu[e]

[a]Sigma Space Corporation, 4801, Forbes Boulevard, Lanham, Maryland 20706
[b]NASA Goddard Space Flight Center (GSFC), Greenbelt, Maryland 20771
[c]Science Systems and Applications, Inc. (SSAI), Lanham, Maryland 20706
[d]NASA GSFC, Greenbelt, Maryland 20771
[e]George Mason University, Global Environment and Natural Resources Institute (GENRI), Department of GGS College of Science, Fairfax, Virginia 20171

Abstract. The objective of this paper is to formulate a methodology to assess the spectral stability of the Libya 4, Libya 1, and Mauritania 2 pseudo-invariant calibration sites (PICS) using Earth Observing One (EO-1) Hyperion sensor. All the available Hyperion collections, downloaded from the Earth Explorer website, were utilized for the three PICS. In each site, a reference spectrum is selected at a specific day in the vicinity of the region of interest (ROI) defined by Committee on Earth Observation Satellites (CEOS). A series of ROIs are predefined in the along-track direction with 196 spectral top-of-atmosphere reflectance values in each ROI. Based on the reference ROI spectrum, the spectral stability of these ROIs is evaluated by average deviations (ADs) and spectral angle mapper (SAM) methods in the specific ranges of time and geo-spatial locations. Time and ROI location-dependent SAM and AD results are very stable within ± 2 deg and $\pm 1.7\%$ of 1σ standard deviations. Consequently, the Libya 4, Mauritania 2, and Libya 1 CEOS selected PICS are spectrally stable targets within the time and spatial swath ranges of the Hyperion collections. © *2014 Society of Photo-Optical Instrumentation Engineers (SPIE)*
[DOI: 10.1117/1.JRS.8.083618]

Keywords: average deviation; calibration; CEOS; Hyperion; Libya 1; Libya 4; Mauritania 2; PICS; RSR; SAM; spectral stability.

Paper 13300P received Aug. 13, 2013; revised manuscript received Mar. 27, 2014; accepted for publication Apr. 10, 2014; published online Jun. 6, 2014.

1 Introduction

Specific locations[1,2] on the Earth's surface with stable radiometric characteristics have been used to evaluate sensors' postlaunch radiometric performance. These pseudo-invariant calibration sites (PICS) have been recommended by the Committee on Earth Observation Satellites (CEOS).[3–5] Most of the CEOS test sites are located in the desert areas with a set of desirable requirements, e.g., spatial uniformity, minimum surface reflectance of 0.3, high signal-to-noise ratio, spectrally flat surface, small seasonal bi-directional reflectance distribution function, near Lambertian surface, and low aerosol loading.[3,6] The CEOS Working Group on Calibration and Validation Infrared and Visible Optical Sensors group recommended a set of test sites for long-term on-orbit radiometric calibration stability of optical imaging sensors. The six CEOS reference PICS are Libya 4, Mauritania 1/2, Algeria 3, Libya 1, and Algeria 5. It should be pointed out that these sites had been used by the Centre National d'Etudes Spatiales for years to calibrate the imaging sensors.[7]

*Address all correspondence to: Taeyoung Choi, E-mail: taeyoung.choi@noaa.gov

0091-3286/2014/$25.00 © 2014 SPIE

Downloaded From: http://remotesensing.spiedigitallibrary.org/ on 04/18/2016 Terms of Use: http://spiedigitallibrary.org/ss/TermsOfUse.aspx

Among these test sites, only Libya 4 and Libya 1 have overlapped Hyperion collections with the CEOS region of interest (ROI). There is no overlap of Hyperion collections with the CEOS ROI for Mauritania 2 site. This site is included in this study because of its broad range of uniformity.

The purpose of this paper is to evaluate the on-orbit spectral stability of the selected CEOS PICS. This paper is an extension of our previous study presented at SPIE. The SPIE work was focused on Libya 4 site only using one Hyperion collection per year from 2004 to 2012.[8] In this study, the developed spectral angle mapper (SAM) and average deviation (AD) methodology is applied to the Libya 4, Mauritania 2, and Libya 1 CEOS PICS. In addition, all the available images, from launch to early of 2013, over the three sites are selected. The Earth Observing One (EO-1) Hyperion response is used as an input to the SAM method which is used to assess the spectral stability of a given target without the gain effect.[9,10] In addition, AD values are calculated to evaluate the spectral variations compared to the reference spectrum.

2 Sensor Overview

As part of a 1-year technology validation/demonstration mission, EO-1 was launched on November 21, 2000. The EO-1 mission was extended thereafter to serve the interest of the scientific community. It has been successfully operated for over 13 years providing hyperspectral measurements. Hyperion on-board, the EO-1 satellite is a push-broom style hyperspectral sensor and its spectral range is from 0.4 to 2.5 μm covered by 242 spectral bands at 10-nm spectral resolution. It has 30-m spatial resolution acquiring measurements over a 7.7-km wide swath.[11]

Out of the 242 spectral bands, the 46 overlapping or noncalibrated bands are not included in this study. Table 1 shows the overlapping and noncalibrated bands.

3 Test Site ROI Information and Hyperion Collections

Cosnefroy et al. identified several radiometrically stable desert targets in the North African and Arabian Desert.[12] An ROI of 100×100 km was chosen to evaluate the spatial uniformity and temporal stability of each site. As mentioned in Sec. 1, there were six CEOS-recommended PICS in the Saharan desert. Only three test sites (Libya 4, Mauritania 2, and Libya 1) are utilized in this study because of the limited swath of EO-1 Hyperion coverage. The Libya 4 site is a high reflectance target located at coordinates of +28.55°N and +23.39°E in the Libyan Desert in the north side of the African continent with an elevation of 118 m above sea level. It is composed of sand dunes with multiple sizes and no signature of vegetation. The second site, Mauritania 2, is located on the northwestern side of the African continent with coordinates centered at +20.85°N and −8.78°E with 384-m altitude. This site has slightly lower reflectance level than the Libya 4 site. The third target, Libya 1, is located at coordinates of +24.42°N and +13.35°E with an altitude of 648 m. It also has various sizes of sand dunes, which become less pronounced in the northwest direction. Additional information on CEOS PICS used in this study is provided in the US Geological Survey (USGS) test site catalog,[13] http://calval.cr.usgs.gov/sites_catalog_map.php, and extensively documented in Ref. 14.

Table 1 Hyperion overlapping and noncalibrated bands.

Band	Wavelength (μm)	Status
1 to 7	0.356 to 0.417	Not calibrated
56 to 57	0.913 to 0.926	Overlaps with 77 to 78
58 to 70	0.936 to 1.058	Not calibrated
71 to 76	0.852 to 0.902	Not calibrated
77 to 78	0.912 to 0.923	Overlaps with 56 to 57
225 to 242	2.406 to 2.578	Not calibrated

Downloaded From: http://remotesensing.spiedigitallibrary.org/ on 04/18/2016 Terms of Use: http://spiedigitallibrary.org/ss/TermsOfUse.aspx

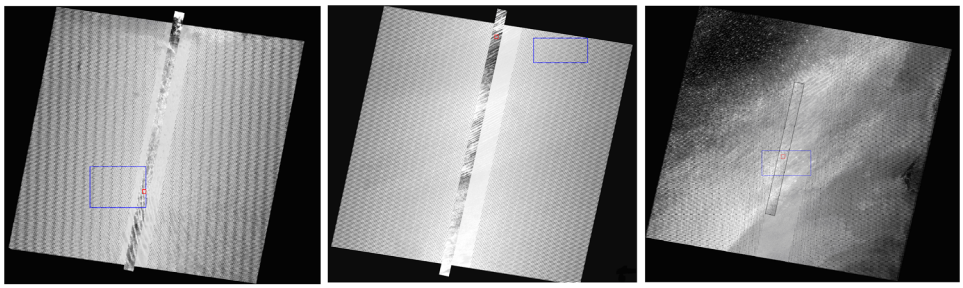

(a) (b) (c)

Fig. 1 Geo-referenced mosaic image of Libya 4, Mauritania 2, and Libya 1 sites using L7 ETM+ band 3 and Hyperion band 16. The blue and red rectangles denote the standard CEOS ROI and Hyperion subset of it as a reference ROI, respectively.

Table 2 The reference ROI coordinates and Hyperion collection dates for the PICS.

Sites	Year	Day	Path	Row	Min. lat.	Min. lon.	Max. lat.	Max. lon.	Area (km^2)
Libya 4	2012	179	181	40	28.55	23.69	28.57	23.72	8.73
Mauritania 2	2012	172	201	46	20.97	−9.11	20.99	−9.08	8.04
Libya 1	2012	167	187	43	24.45	13.34	24.48	13.37	8.82

To visualize the differences between CEOS specification and the reference ROI, the geo-located images are shown in Fig. 1 using Enhanced Thematic Mapper Plus (ETM+) and Hyperion collections. The Hyperion scenes have a very narrow swath of 7.7 km compared to ETM+'s 187-km swath. In Fig. 1(a), the Libya 4 CEOS ROI is illustrated by a blue rectangular box, whereas the reference ROI is represented by a small red box within the Hyperion overlap. The ETM+ images included in Fig. 1 are for visualization purposes only.

The Landsat World Reference System 2 path/row and latitude/longitude coordinate information for these reference ROIs are shown in Table 2. These ROIs will be used as a baseline for further spectral stability analysis along with other ROIs. For the Mauritania 2 site, the location of the CEOS ROI is not included by the Hyperion collection. However, the Hyperion reference ROI is close enough to the PICS ROI and spectral signatures are very similar so that we can define the reference ROI as shown in Fig. 1(b). On the other hand, the reference ROIs in Libya 4 and Libya 1 sites are the subsets of the CEOS ROIs as shown in Fig. 1(c). The further details of spectral similarities between the CEOS and reference ROI are discussed in Sec. 5.

4 Data Processing and Methodology

The EO-1 Hyperion data are readily available through USGS Earth Explorer website at http://earthexplorer.usgs.gov/. In this study, the processing level of the Hyperion data is Level 1Gst, which is radiometrically corrected and resampled for geometric correction and registration to a geographic map projection. All available images of the three sites were selected from launch to early 2013. Prior to cloud filtering, a total of 302 Hyperion scenes were available with Libya 4 site since 2004. There were 118 and 19 scenes available for Mauritania 2 and Libya 1 sites, respectively. Table 3 provides a summary of the total number of scenes used in our analysis. All these scenes were processed to compute the TOA reflectance before performing further analyses.

4.1 *Conversion to TOA Reflectance*

As an initial step, the pixel calibrated digital numbers (DNs) need to be corrected for rescaling gain/bias and converted to absolute radiometric units such as at-sensor radiance or TOA

Downloaded From: http://remotesensing.spiedigitallibrary.org/ on 04/18/2016 Terms of Use: http://spiedigitallibrary.org/ss/TermsOfUse.aspx

Table 3 Summary of number of scenes per year for Libya 4, Mauritania 2, and Libya 1 from year 2003 to 2013.

Year	03	04	05	06	07	08	09	10	11	12	13
Libya 4	N/A	14	9	30	48	54	47	27	23	42	8
Mauritania 2	3	10	4	21	15	18	11	11	9	14	1
Libya 1	N/A	N/A	N/A	N/A	N/A	N/A	N/A	N/A	N/A	18	N/A

reflectance. The Hyperion DNs are converted to TOA reflectance values using the information provided in the metafile. The at-sensor radiance and reflectance (ρ_λ) calculations are performed using the standard equation

$$\rho_\lambda = \frac{\pi \cdot L_\lambda \cdot d^2}{\mathrm{ESUN}_\lambda \cdot \cos\theta_s}. \tag{1}$$

The reflectance (ρ_λ) is proportional to the spectral radiance at the sensor's aperture (L_λ) and the square of the Earth–sun distance (d) in astronomical units divided by the mean exoatmospheric solar irradiance (ESUN_λ) and cosine of the solar zenith angle (θ_s) Hyperion ESUN_λ is calculated based on Thullier model[15] and the TOA reflectance values are integrated over the active wavelength range defined by the RSR.

4.2 *Selection of Hyperion ROIs*

A reference rectangular ROI (approximately 2.9×2.9 km) was defined for each test site by the latitude and longitude ranges as specified in Table 2. As an example, the Libya 4 test site reference ROI is shown as a small red rectangle in Fig. 1, which is a subset of the CEOS PICS. Based on the reference ROI, additional ROIs are selected along the EO-1 satellite track direction as shown in Fig. 2(a). In each test site, the reference ROI is marked as a dark shaded rectangle corresponding to the number "0." The Hyperion spectrum from ROI 0 is used as a reference spectrum, which is further used to compare against the spectra from other ROIs. Other rectangular ROIs are defined in Fig. 2 along the track direction of the satellite. Average reflectance is computed for each ROI on a band-by-band basis using the mean value. The spectra derived from each ROI are compared with the reference spectra to assess the spatial stability of the test sites. If there is any fill or saturated pixel value within any ROI, it is excluded in the reflectance calculation.

4.3 *Average Deviation*

Once all the ROI spectra are retrieved, the spectral similarity of the selected ROI can be assessed by measuring the reflectance differences between the reference ROI and the other testing ROIs using all the Hyperion spectral bands. To evaluate the reflectance differences in all the bands, the normalized average absolute deviation (i.e., AD) is calculated by taking the sum of absolute difference between the reference spectrum and testing spectra normalized by the number of bands. Sometimes, median values are used as a robust estimator in median absolute deviation because of its little computation time and simple formula.[16] In this study, mean values are calculated in the reference and testing ROIs to keep the AD values in the reflectance compatible scale. This AD provides an estimate of the site's variability as a summary statistics of statistical dispersion across all wavelengths

$$\mathrm{AD} = \frac{1}{\mathrm{nb}} \sum_{i=1}^{\mathrm{nb}} |r_i - t_i|, \tag{2}$$

where nb is the number of bands, r is the reference spectrum, and t is the testing spectrum.

Downloaded From: http://remotesensing.spiedigitallibrary.org/ on 04/18/2016 Terms of Use: http://spiedigitallibrary.org/ss/TermsOfUse.aspx

Fig. 2 True color images of the test sites using Hyperion bands 30, 24, and 16 for red, green, and blue (RGB) compositions, respectively. The ROI "0" is the reference ROI. All other ROIs are selected based on the coverage of the Hyperion collections.

4.4 *Spectral Angle Mapper*

The SAM has been used to identify a material by measuring the spectral similarity to a reference spectrum in multispectral and hyperspectral images. SAM is used as a measure of spectral similarity to identify a material for classification.[9] Also, it has been used for geological mapping and identifying the minerals on the ground by referring to the USGS Spectral Library to detect mine waste.[17]

The reference spectra could be either remotely sensed data or laboratory measurements. The main advantage of the SAM is that it reduces "apparent reflectance" of the different illumination or shade effects. The SAM algorithm only uses the spectral angle between testing spectra and reference spectra by treating reflectance values from different bands as vectors. The measured angle between the reference and testing spectra is calculated as follows:[9,10]

Downloaded From: http://remotesensing.spiedigitallibrary.org/ on 04/18/2016 Terms of Use: http://spiedigitallibrary.org/ss/TermsOfUse.aspx

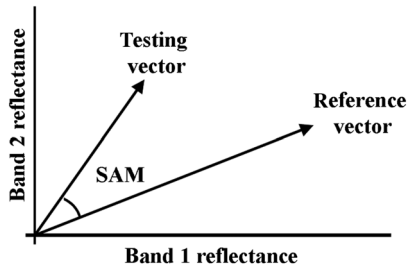

Fig. 3 The concept of spectral angle mapper (SAM) using a simple sensor with two bands.

$$\mathrm{SAM} = \cos^{-1}\left(\frac{\vec{t}\cdot\vec{r}}{\|\vec{t}\|\cdot\|\vec{r}\|}\right) = \cos^{-1}\left(\frac{\sum_{i=1}^{\mathrm{nb}} t_i \cdot r_i}{\sqrt{\sum_{i=1}^{\mathrm{nb}} t_i^2}\cdot\sqrt{\sum_{i=1}^{\mathrm{nb}} r_i^2}}\right). \tag{3}$$

The SAM computes a spectral angle between the testing and reference spectrum. For a simple case, an SAM angle is illustrated in Fig. 3 from two band responses as shown as test and reference vectors. When a vector is drawn from the origin through each response in bands 1 and 2, the angle between these two vectors constructs the SAM. The smaller the SAM angle, the more similar the reference and testing spectra. This spectral angle is insensitive to changes in the ROI illumination (or magnitude), because the increase or decrease of the reflectance levels is not affecting the angles of the reference or testing vectors as shown in Fig. 3.

5 Results and Analysis

As noted in Table 3, temporal coverage of Libya 4 and Mauritania 2 sites is quite well distributed in last 10 years, whereas only 18 scenes exist in 2012 with the Libya 1 site. Our spectral stability analysis starts from Libya 4 because there are many scenes available compared to other sites. The total numbers of available Hyperion scenes are 302 and 117 for Libya 4 and Mauritania 2 sites, respectively.

For each testing site, an initial usable range of ROIs is checked compared to the reference ROI with the reference collection (as defined in Table 2) excluding the apparently nonuniform ROIs with different ground spectra in the EO-1s along-track direction. Once the usable ROI ranges are checked, the time and ROI location-dependent spectral stabilities are estimated.

5.1 *Spectra Comparisons on the Reference Hyperion Collection*

This section provides detailed comparisons between the reference spectrum from the reference collection and the other spectra from other testing ROIs. For each site, a reference Hyperion collection is defined in Table 4. This spectrum from the reference ROI on the reference collection is being used for all the following spectral analyses with AD and SAM methods. The total number of the ROIs including the reference and testing ROIs, mean longitude, latitude range, and approximate ROI coverage in kilometers are shown in Table 4. The number of ROI and approximate along-track ROI coverages in the Mauritania 2 is almost twice as large as that of Libya 1,

Table 4 The total number of ROIs, mean longitude, latitude range, and approximate ROI coverage in kilometers from the reference Hyperion collection.

Sites	Year	Day	Number of ROI	Mean lon.	Lat. range	Approximate ROI coverage (km)
Libya 4	2012	179	59	23.782	28.072 to 29.500	170
Mauritania 2	2012	172	62	−9.262	19.364 to 21.134	204
Libya 1	2012	167	30	13.378	24.099 to 24.981	104

Downloaded From: http://remotesensing.spiedigitallibrary.org/ on 04/18/2016 Terms of Use: http://spiedigitallibrary.org/ss/TermsOfUse.aspx

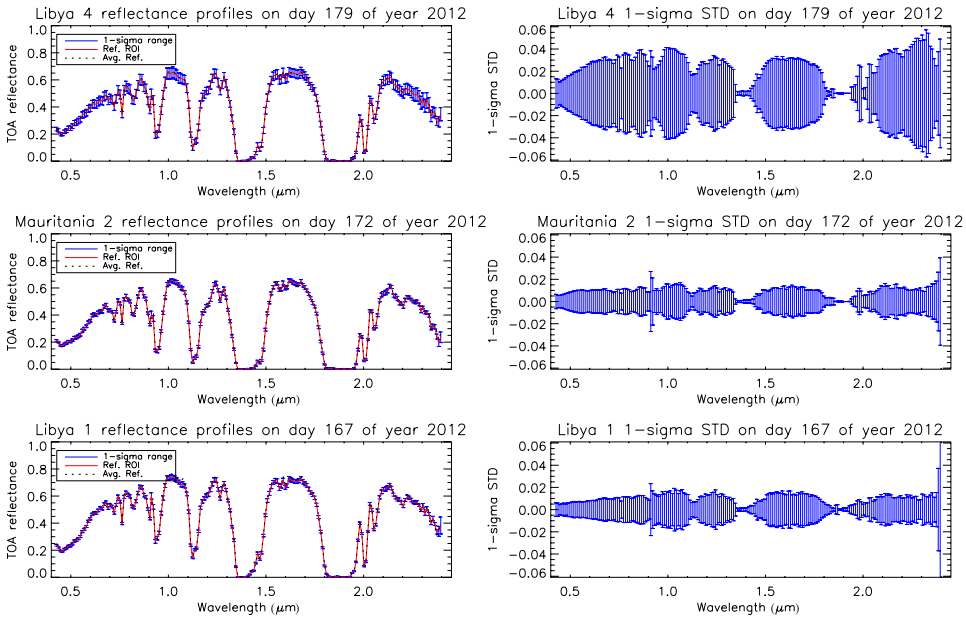

Fig. 4 Mean and 1σ standard deviation of the Hyperion spectral reflectance responses from all the ROIs with the reference collection.

which is also shown in Fig. 2. These differences are caused by the duration of Hyperion collections. In each ROI, there are 196 reflectance values corresponding to each spectral band ranging from 0.425 to 2.395 μm at a spectral resolution of 10 nm. Figure 4 shows the mean values and 1σ standard deviation ranges as error bars using all the spectra from all the ROIs. The red solid line is the reference spectrum with index "0" from Fig. 2 and averaged profile is shown as dashed black line. In the first column of Fig. 4, there are common atmospheric absorption features in the Hyperion spectral range with some spectral intensity deviations especially in Libya 4 site.

To effectively visualize these differences, 1σ standard deviation plots are generated using all the ROIs in the second column of Fig. 4. The standard deviations are calculated based on the reflectance difference from the reference spectrum in each ROI. The Libya 4, Mauritania 2, and Libya 1 sites are showing spectral similarities between the reference ROI and other ROIs within $\pm 5\%$ of the reflectance difference except some longwave length bands. In addition, the Libya 4 site's spectra are slightly larger values than other sites, which are caused by the different ground materials as shown in Fig. 1 on top of the Hyperion collection. These location-dependent outliers are rejected and the method will be discussed in the following section.

5.2 *Spectral Stability from AD and SAM on the Reference Hyperion Collection*

Since there are some outlier points especially in the Libya 4 sites, the AD and SAM values are calculated for all the ROIs using the reference Hyperion collection to check specific spectrum deviation compared to the reference spectrum. The AD and SAM values represent the reflectance differences and vector angle differences observed across the 196 Hyperion spectral bands. In Fig. 5, the AD and SAM values are zero (denoted by the green diamond symbols), because all the AD and SAM results are calculated based on the same reference ROI. The x-axis of the figures is based on the center latitudes of the ROIs. The AD values are compatible with the average reflectance differences over all the bands by its definition from Eq. (2). In the Libya 4 site, the AD values beyond the $+29.5$ deg latitude show a significant upward trend. Generally, the AD results are very stable and mostly <0.03 in Fig. 5 and Table 5. The AD values beyond the $+29.5$ deg latitude show a significant upward trend in both AD and SAM results, further confirming that the spectra of these ROIs are different in comparison to the reference ROI. The ROIs beyond the latitude limit of 29.5 deg will not be considered in further AD and SAM results. The Libya 4 outlier profiles in Fig. 4 are caused by the sudden spikes near the latitudes of 29.0 and 28.2, which have higher reflectance differences compared to the reference ROI. Regardless of the

Downloaded From: http://remotesensing.spiedigitallibrary.org/ on 04/18/2016 Terms of Use: http://spiedigitallibrary.org/ss/TermsOfUse.aspx

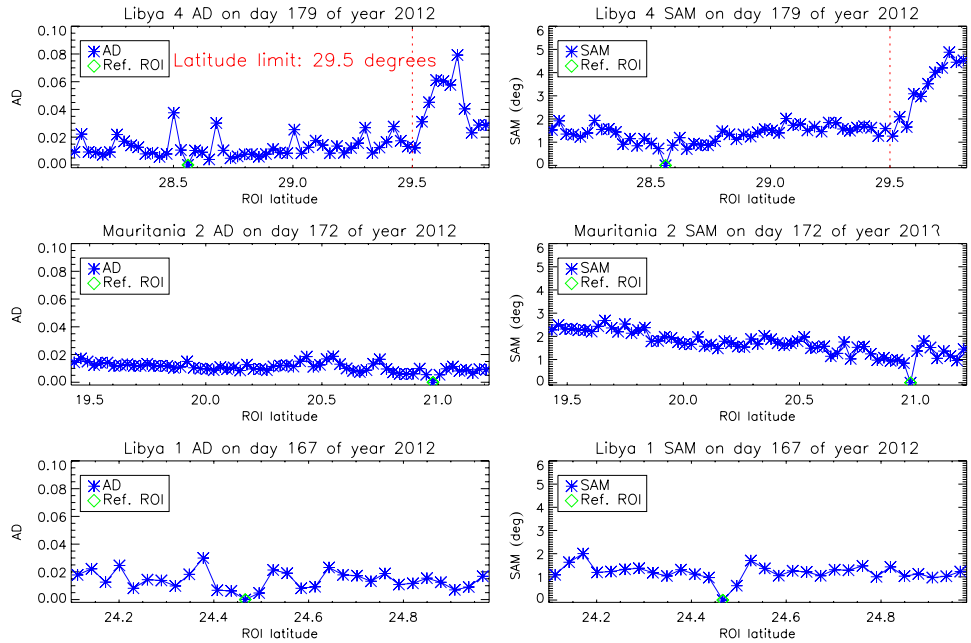

Fig. 5 The AD and SAM results using all the bands in a Hyperion collection.

reflectance differences, the ground spectral compositions of the outlier ROIs are very consistent with that of the reference ROI because the SAM responses remained stable. The SAM values are gradually decreased in the Mauritania 2 site. The mean and STD values are higher than other sites; however, the degree of SAM value change is <0.5 compared to the other sites and the AD shows as very stable in Table 5. Consequently, all the three testing sites are spectrally uniform with small variations in AD and SAM values, <0.03 and 3 deg, respectively.

5.3 *Time-Dependent Spectral Stability and Cloudy Scene Filtering*

Figure 6 shows the time series SAM and AD results without applying any filtering. Apparently there are some cloudy scenes, which produced very large differences up to 40 deg with SAM and 0.35 with AD values. In this AD and SAM analysis, all the 198 bands' reflectance values are applied without separating ETM+ band ranges. Figure 6 shows all the SAM and AD values in Libya 4 site from year 2003 to 2013 with days from 2003, i.e., "Ep 2003" in the x-axis. In each Hyperion collection or a specific location in the plot, there are approximately 60 points from the number of ROIs for the Libya 4 site. Whenever a collection was made on a clear cloud-free day, the SAM and AD values are <10 and 0.1, which was based on the visual check with natural color images. Especially in Fig. 6, the SAM and AD values were <10 deg and 0.1 with the clear day collections near the day 400 and 4000 in the x-axis. On the contrary, the SAM value reached at

Table 5 The mean and standard deviation values of AD and SAM.

	Result			
	AD (reflectance)		SAM (deg)	
Sites	Mean	STD	Mean	STD
Libya 4[a]	0.013	0.007	1.345	0.388
Mauritania 2	0.011	0.003	1.695	0.502
Libya 1	0.014	0.007	1.186	0.342

[a]Libya 4 results are calculated from the ROIs <29.5 deg.

Downloaded From: http://remotesensing.spiedigitallibrary.org/ on 04/18/2016 Terms of Use: http://spiedigitallibrary.org/ss/TermsOfUse.aspx

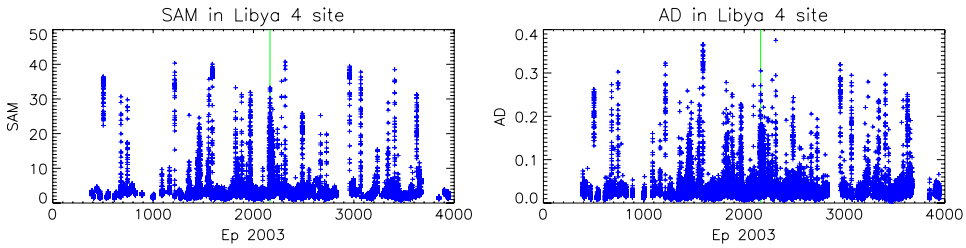

Fig. 6 The Libya 4 AD and SAM results using all the bands from Hyperion collections in years from 2004 to 2013.

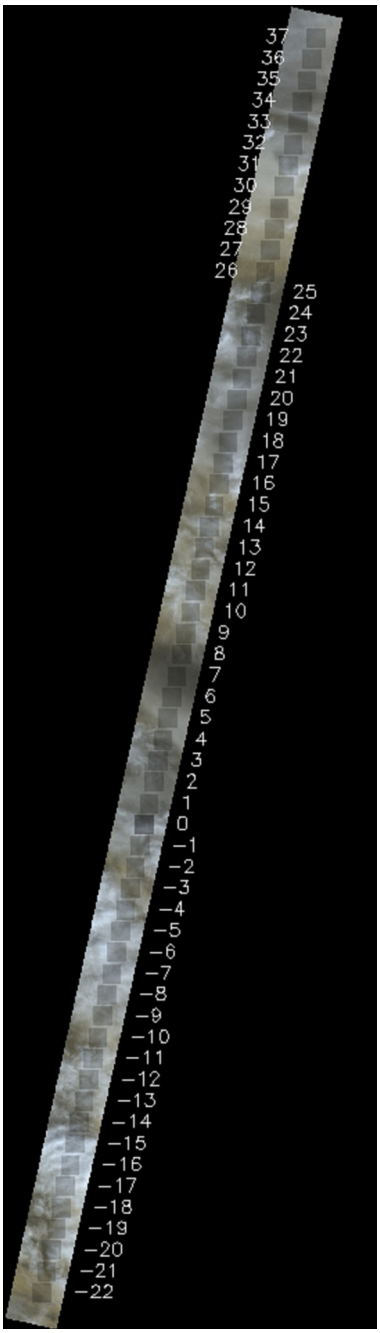

Fig. 7 A cloudy collection on day 338 in the year 2008. A true color images is generated using Hyperion bands 30, 24, and 16 for RGB.

Downloaded From: http://remotesensing.spiedigitallibrary.org/ on 04/18/2016 Terms of Use: http://spiedigitallibrary.org/ss/TermsOfUse.aspx

33 deg with an extremely cloud day as indicated as a green line in Fig. 6 collected on day 338 in year 2008. The color image of the collection is also shown in Fig. 7. The corresponding AD value also went up to 0.3. From these observations, cloudy conditions are detected by the threshold SAM and AD values of 10 and 0.1. This means that whenever there is a larger SAM value of 10 deg or AD value of 0.1 in one of the ROIs in a given day, the whole scene is defined as a cloudy scene and it is excluded for further analyses. There are 22 cloudy Hyperion collections detected for Libya 4 site from 2003 to 2013 as shown in Table 6. The mean value of the maximum SAM value is approximately 26 deg with large variation range from 8.06 up to 40.33 deg. Along with these SAM values, AD values are mostly higher than 0.1 in the reflectance scale and they are highly correlated with each other. Figure 8 shows the filtered SAM and AD results after the cloudy filtering of the Libya 4 site. The green solid lines and numbers in the background indicate the year division point.

However, the threshold of the SAM is set to be 10 deg, all the values are <8 deg after the filtering. Similarly, AD values are mostly under 0.08 except some noisy ROIs. The same cloudy scene detection and filtering method are applied to the Mauritania 2 and Libya 1 sites, respectively. The total numbers of Hyperion collections and cloudy scenes are listed in Table 7. The mean and standard deviation values of the SAM and AD are also summarized in Table 7.

Table 6 Maximum SAM and AD values for Libya 4 cloudy scenes.

Number	Year	DOY	Max. SAM	Max. AD
1	2004	138	36.41	0.26
2	2004	314	30.65	0.27
3	2005	12	29.75	0.30
4	2005	356	9.63	0.16
5	2006	118	40.33	0.32
6	2006	347	15.04	0.16
7	2006	362	24.54	0.18
8	2007	7	17.81	0.14
9	2007	128	40.04	0.37
10	2007	360	33.25	0.28
11	2008	8	12.58	0.20
12	2008	59	17.56	0.20
13	2008	105	17.20	0.11
14	2008	141	31.90	0.23
15[a]	2008	338	33.18	0.30
16	2008	353	23.71	0.18
17	2008	366	26.97	0.22
18	2011	35	39.45	0.32
19	2011	146	37.74	0.29
20	2011	286	8.06	0.22
21	2012	46	14.16	0.23
22	2012	339	31.26	0.25

[a]This collection is shown as a green line in Fig. 6.

Downloaded From: http://remotesensing.spiedigitallibrary.org/ on 04/18/2016 Terms of Use: http://spiedigitallibrary.org/ss/TermsOfUse.aspx

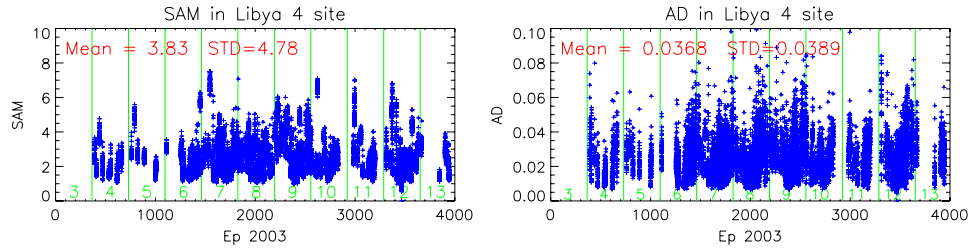

Fig. 8 The Libya 4 AD and SAM results using all the bands in a Hyperion collections.

The Libya 1 site provides the most stable SAM and AD results; however, the number of Hyperion collections is significantly smaller than other sites. It is not statically fair comparing with other sites because of the small number of collections but Libya 1 site provides very stable spectral results from the SAM and AD results over a year range.

The Libya 4 site also provides very stable and similar results to the Libya 1 site, even though the Libya 4 results are calculated from a larger number of scenes. The mean SAM angle difference is 2.52 with very tight standard deviation value of 1.06. The AD result is also very small mean value of 2.6% with 1.2% standard deviation in the reflectance scale. The Libya 4 site produces slightly higher mean and standard deviation in SAM and AD analysis than the results from the Libya 1 site, but both sites are still a spectrally very stable and having similar stabilities when interannual variations are considered.

After the cloudy scene rejection filtering, there are 117 Hyperion collections used. Over a decadal analysis, the rate of cloudy scene is approximately two times higher than Libya 4 site. In conjunction to the atmospheric condition, the mean and standard deviation values are larger than the two Libyan sites as shown in Table 7. The difference in the mean value suggests the constant angle or reflectance offset compared to the reference spectrum. The actual stabilities in the SAM and AD are captured by the standard deviations. The SAM standard deviation increase rate from Libya 4 to Mauritania 2 sites is from 1.06 to 1.99 deg, which is 87.7% increase. In the same way, the AD increase rate is 33.3%. From these two increase rates, the SAM technique is more sensitive than the AD method.

5.4 *ROI Location-Dependent Spectral Stability Estimations*

Besides the temporal analysis, ROI location-based spectral stability of the selected testing sites is also evaluated using the cloud-filtered Hyperion collections. Due to different start time of each Hyperion granule, slightly varying ROI coverages are obtained in the along-track direction. A common latitude range is chosen for each site as shown in Fig. 2. The ROIs above 29.5 deg are not included in Libya 4 site as mentioned earlier, which reduced about 11 ROIs above the latitude limit. For the Libya 4 and Mauritania 2 sites, 10-year collections are used to calculate mean and standard deviation of SAM and AD for each ROI location, respectively. For the Libya 1 site, only 1 year collations in 2012 are used. Figure 9 shows SAM and AD results at the center latitudes of the ROIs in the x-axis. In all sites, the mean SAM angles are very stable at specific average levels

Table 7 SAM and AD results in Libya 4, Mauritania 2, and Libya 1 sites with cloud rejection filtering.

Site	Libya 4	Mauritania 2	Libya 1
Time range	2004 to 2013	2003 to 2012	2012
Number of scenes	302	117	19
Number of cloudy scene	22	18	2
Lifetime SAM mean $\pm 1\sigma$	2.51 ± 1.06	4.12 ± 1.99	2.24 ± 0.77
Lifetime AD mean $\pm 1\sigma$	$2.6\% \pm 1.2\%$	$3.2\% \pm 1.6\%$	$2.6\% \pm 1.1\%$

Downloaded From: http://remotesensing.spiedigitallibrary.org/ on 04/18/2016 Terms of Use: http://spiedigitallibrary.org/ss/TermsOfUse.aspx

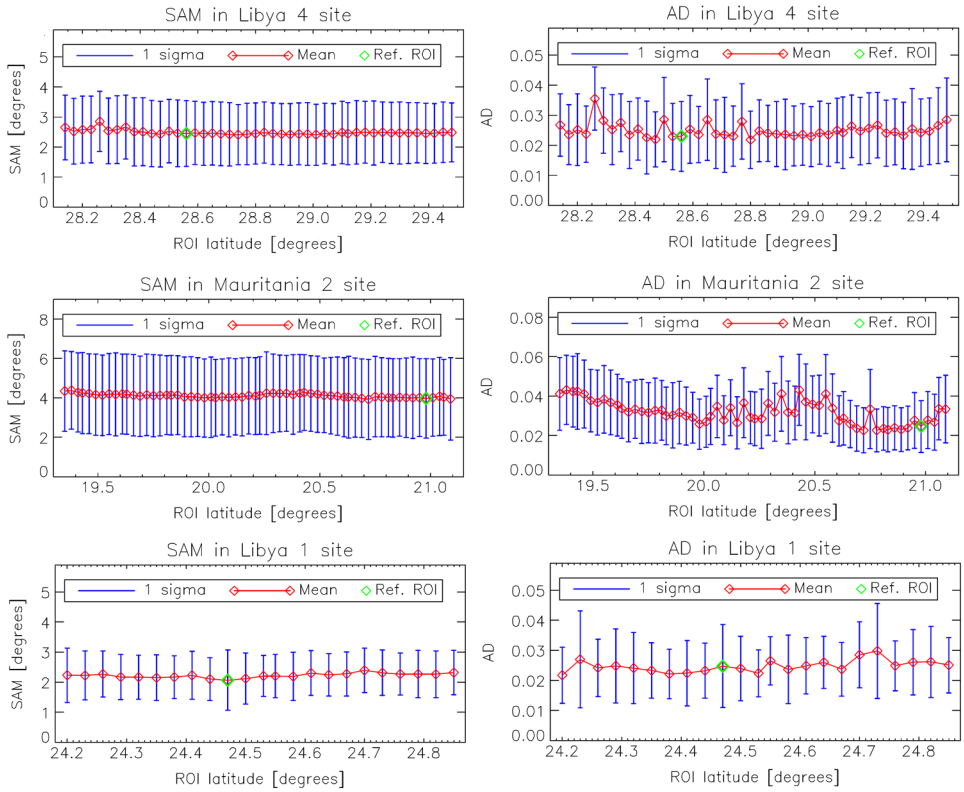

Fig. 9 ROI location based spectral stability from SAM and AD methods. The error bars represent the 1σ range and the green diamond symbol represents the reference ROI location in the specific site.

Table 8 Average of SAM mean, SAM STD, AD mean, and AD STD for Libya 4, Mauritania 2, and Libya 1 sites after cloud-rejection filtering.

Site	Average			
	SAM mean	SAM STD	AD mean	AD STD
Libya 4	2.49	1.05	0.0249	0.0111
Mauritania 2	4.11	2.00	0.0319	0.0150
Libya 1	2.22	0.77	0.0248	0.0105

from all the ROIs. The maximum differences in the averaged SAM angles from all the ROIs are 0.44, 0.46, and 0.33 deg in Libya 4, Mauritania 2, and Libya 1 site, respectively. The corresponding maximum differences with the averaged AD values are 1.37%, 2.05%, and 0.81%. The average of SAM mean, SAM STD, AD mean, and AD STD values are angles of the two Libyan sites are summarized in Table 8. Under the condition that the average of mean SAM is just showing a stable and constant offset from the reference spectrum, the average of SAM STD represents level of stability over the testing period. Over the 10 years of collections, the averaged STD value of the Libya 4 site is 0.95 deg less than Mauritania 2 site. As a result of it, mean AD trending in this site showing larger variation along with the track direction ROIs in Fig. 9. The mean of STD result in the Mauritania 2 site is also higher than other two Libyan sites in Table 8. Even though the Mauritania 2 site shows higher variations in SAM and AD results, overall ROI spectral stability is excellent in SAM analysis with very stable and mean and STD results with very small variations in all the three testing sites. As a cross validation, the location dependent results shown in Table 8 are very similar to the time-dependent results with Table 7.

Downloaded From: http://remotesensing.spiedigitallibrary.org/ on 04/18/2016 Terms of Use: http://spiedigitallibrary.org/ss/TermsOfUse.aspx

6 Conclusion

The on-orbit spectral stability of the selected CEOS PICS (Libya 4, Mauritania 2, and Libya 1) is evaluated by using hyperspectral collections from EO-1 Hyperion. Ten years of Hyperion collections over Libya 4 and Mauritania 2 sites, and 1-year collections over the Libya 1 site, were processed. A set of ROIs with a dimension of 2.9×2.9 km are defined in the satellite track direction in each site. A reference ROI is selected in the year 2012 which is a smaller subset or near of the CEOS target ranges and it is served as the baseline spectrum to estimate spectral stability using the AD and SAM methods.

Within the Libya 4 site, the ROIs below 29.5-deg latitude are used because of the rapid ground spectra changes above the limit. Cloud-contaminated scenes are identified and filtered by the SAM and AD threshold values of 10 deg and 0.1, respectively, in the three sites. The time-dependent SAM and AD values are very stable mostly within ± 2.0 deg and $\pm 1.7\%$ in the reflectance scale, when the standard deviations are considered at constant mean levels. The ROI location-dependent results are very stable over the testing period in all three sites. The maximum variation ranges of the SAM and AD values are very small within 0.5 deg and 2.5%. It also suggests the limited spatial stability along the narrow swath of the Hyperion track direction is very stable in terms of SAM and AD. The mean of location-dependent SAM and AD 1σ standard deviations are within ± 2.0 deg and $\pm 1.5\%$. Consequently, the Libya 4, Mauritania 2, and Libya 1 sites are spectrally very stable targets within ± 2 deg of SAM and $\pm 1.7\%$ of AD 1σ standard deviation from all the available Hyperion collections and different ROI locations at a stable mean levels.

References

1. G. Chander et al., "Online catalogue of world-wide test sites for the post-launch characterization and calibration of optical sensors," in *Int. Astronautical Federation—58th Int. Astronautical Congress*, Paris, France, pp. 2043–2051 (2007).
2. G. Chander et al., "An assessment of African test sites in the context of a global network of quality-assured reference standards," in *IEEE Int. Geoscience and Remote Sensing Symposium 2009 (IGARSS 2009)*, Piscataway, New Jersey, Vol. 5, pp. 236–239 (2009).
3. P. M. Teillet and G. Chander, "Terrestrial reference standard sites for postlaunch sensor calibration," *Can. J. Remote Sens.* **36**(5), 437–450 (2010), http://dx.doi.org/10.5589/m10-079.
4. G. Chander et al., "Preliminary assessment of several parameters to measure and compare usefulness of the CEOS reference pseudo-invariant calibration sites," *Proc. SPIE* **7826**, 78262L (2010), http://dx.doi.org/10.1117/12.865166.
5. P. Campbell et al., "EO-1 hyperion reflective time series at calibration and validation sites: stability and sensitivity to seasonal dynamics," *IEEE J. Sel. Top. Appl. Earth Obs. Remote Sens.* **6**(2), 276–290 (2013), http://dx.doi.org/10.1109/JSTARS.2013.2246139.
6. P. Teillet et al., "Prime candidate earth targets for the post-launch radiometric calibration of space-based optical imaging instruments," *Proc. SPIE* **6677**, 66770S (2007), http://dx.doi.org/10.1117/12.733156.
7. S. Lacherade et al., "Cross calibration over desert sites: description, methodology, and operational implementation," *IEEE Trans. Geosci. Remote Sens.* **51**(3), 1098–1113 (2013), http://dx.doi.org/10.1109/TGRS.2012.2227061.
8. T. Choi et al., "Spectral stability of the Libya 4 site using EO-1 Hyperion," *Proc. SPIE* **8724**, 872410 (2013), http://dx.doi.org/10.1117/12.2016644.
9. F. A. Kruse et al., "The spectral image processing system (SIPS)—interactive visualization and analysis of imaging spectrometer data," *Remote Sens. Environ.* **44**(2–3), 145–163 (1993), http://dx.doi.org/10.1016/0034-4257(93)90013-N.
10. R. H. Yuhas, A. F. H. Goetz, and J. W. Boardman, "Discrimination among semiarid landscape endmembers using the spectral angle mapper (SAM) algorithm," in *Summaries of the Third Annual JPL Airborne Geoscience Workshop*, Vol. 1, pp. 147–149, JPL Publication, Pasadena, California (1992).
11. E. Middleton et al., "The Earth Observing One (EO-1) satellite mission: over a decade in space," *IEEE J. Sel. Top. Appl. Earth Obs. Remote Sens.* **6**(2), 243–256 (2013), http://dx.doi.org/10.1109/JSTARS.2013.2249496.

Downloaded From: http://remotesensing.spiedigitallibrary.org/ on 04/18/2016 Terms of Use: http://spiedigitallibrary.org/ss/TermsOfUse.aspx

12. H. Cosnefroy, M. Leroy, and X. Briottet, "Selection and characterization of Saharan and Arabian Desert sites for the calibration of optical satellite sensors," *Remote Sens. Environ.* **58**(1), 101–114 (1996), http://dx.doi.org/10.1016/0034-4257(95)00211-1.
13. G. Chander et al., "Online catalog of world-wide test sites for the post-launch characterization and calibration of optical sensors," in *Proc. 58th Int. Astronautical Congr.*, Hyderabad, India, pp. 2043–2051 (2007).
14. S. Lachérade et al., "Cross-calibration over desert sites: description, methodology and operational implementation," *IEEE Trans. Geosci. Remote Sens.* **51**(3), 1098–1113 (2013), http://dx.doi.org/10.1109/TGRS.2012.2227061.
15. G. Thuillier et al., "The solar spectral irradiance from 200 to 2400 nm as measured by the SOLSPEC spectrometer from the ATLAS and EURECA missions," *Solar Phys.* **214**(1), 1–22 (2003), http://dx.doi.org/10.1023/A:1024048429145.
16. P. J. Rousseeuw and C. Croux, "Alternatives to the median absolute deviation," *J. Am. Stat. Assoc.* **88**(424), 1273–1283 (1993), http://dx.doi.org/10.1080/01621459.1993.10476408.
17. I. McCubbin et al., "Mineral mapping using partial unmixing at ray mine, AZ," in *7th Annual Airborne Earth Science Workshop*, Pasadena, California (1998).

Taeyoung Choi received a BS degree in electronics from Kon-Kuk University in the Republic of Korea and an MS degree in electrical engineering at South Dakota State University, USA. He is a PhD candidate at George Mason University and currently works for NOAA performing radiometric calibrations for S-NPP VIIRS with ERT Corp. He has been working in remote sensing, instrument calibration, and data applications since 1999 with sensors such as IKONOS, QuickBird, ETM+, ALI, Hyperion, MODIS, and VIIRS.

Xiaoxiong Xiong is an optical physicist at NASA Goddard Space Flight Center (GSFC). He is currently serving as the MODIS project scientist and the technical lead for the MODIS Characterization Support Team (MCST) and the VIIRS Calibration Support Team (VCST). In addition to sensor calibration, He had also worked in the fields of optical instrumentation, nonlinear optics, laser and atomic spectroscopy, and resonance ionization mass spectrometry.

Amit Angal received an MS degree in electrical engineering from South Dakota State University, Brookings, South Dakota. He is currently a senior instrument engineer with Science Systems and Applications, Inc., primarily working with on the radiometric characterization and calibration of the reflective solar bands of the MODIS instruments on board the Terra and Aqua spacecrafts. His research interests include sensor cross-calibration and validation.

Gyanesh Chander received the PhD in geospatial science and engineering with specialization in remote sensing engineering, and an MS degree in electrical engineering from South Dakota State University, Brookings. He joined the NASA GSFC in Greenbelt, Maryland, to support the Joint Polar Satellite System Ground Project as the data products engineering and services manager. Previously, he served as a principal systems engineer with SGT, Inc., at the USGS Earth Resources Observation and Science Center in South Dakota.

John J. Qu is a professor in the College of Science at George Mason University, USA. He is the founder and director of the Global Environment and Natural Resources Institute (GENRI) and Environmental Science and Technology Center, at GMU. He received PhD and MS degrees from Colorado State University and a BS degree from Nanjing Institute of Meteorology, China. His research areas are satellite remote sensing, atmospheric radiation transfer, environment sciences, and sustainable energy geo-information system applications.

Downloaded From: http://remotesensing.spiedigitallibrary.org/ on 04/18/2016 Terms of Use: http://spiedigitallibrary.org/ss/TermsOfUse.aspx